Coupled Heat and Mass Transfer By MHD Free Convection Flow along a Vertical Plate with Streamwise Temperature and Species Concentration Variations

Ali J. Chamkha,[1] S.M.M. EL-Kabeir,[2,3] and A.M. Rashad[2]
[1]Manufacturing Engineering Department, The Public Authority for Applied Education and Training, Shuweikh, Kuwait
[2]Department of Mathematics, Faculty of Science, South Valley University, Aswan, Egypt
[3]Department of Mathematics, Salman bin Abdulaziz University, College of Science and Humanity Studies, Al-Kharj, Saudi Arabia

The problem of steady, laminar, coupled heat and mass transfer by MHD free convective boundary-layer flow along a vertical flat plate with the combined effects of streamwise sinusoidal variations of both the surface temperature and the species concentration in the presence of Soret and Dufour effects is considered. A suitable set of dimensionless variables is used to transform the governing equations of the problem into a non-similar form. The resulting non-similar equations have the property that they reduce to various special cases previously considered in the literature. An adequate and efficient implicit, tri-diagonal finite difference scheme is employed for the numerical solution of the obtained equations. Various comparisons with previously published work are performed and the results are found to be in excellent agreement. A representative set of numerical results for the velocity, temperature, and concentration profiles as well as the surface shear stress, rate of heat transfer, and the rate of mass transfer is presented graphically for various parametric conditions and is discussed. Heat Trans Asian Res, 42(2): 100–110, 2013; Published online 28 December 2012 in Wiley Online Library (wileyonlinelibrary.com/journal/htj). DOI 10.1002/htj.21033

Key words: heat and mass transfer, MHD, natural convection, Soret and Dufour effects, sinusoidal surface temperature and concentration

1. Introduction

Coupled heat and mass transfer finds applications in a variety of engineering applications, such as the migration of moisture through the air contained in fibrous insulation, grain storage installations, filtration, and chemical catalytic reactors, and in processes such as spreading of chemical pollutants in plants and diffusion of medicine in blood veins. Free convection flow of an incompressible viscous fluid past an infinite or semi-infinite vertical plate has been studied so long because of its technological importance. Many studies that considered combined heat and mass transfer in natural convection boundary-layer flows over heated surfaces with various geometries can be found in the monograph by Gebhart el al. [1]. Callahan and Marner [2] solved the problem of transient free convection with mass transfer on an isothermal vertical plate using an explicit finite difference scheme. Unsteady free convective flow taking into account the mass transfer phenomenon past an infinite vertical porous plate with constant suction was studied by Soundalgekar and Wavre [3]. Soundalgekar [4] studied the effects of mass transfer and free convection currents on the flow past an impulsively started vertical plate. In these studies, the magnetohydrodynamic effect is ignored. However, in metallurgical transport systems, by drawing plates in an electrically conducting fluid subjected to a transverse magnetic field, the rate of cooling can be controlled and the final desired characteristics can be further refined. Magnetohydrodynamic flows have applications in meteorology, solar physics, cosmic fluid dynamics, astrophysics, geophysics, and in the motion of the earth's core. Shanker and Kishan [5] presented the effect of mass transfer on the MHD flow past an impulsively started infinite vertical plate. Chamkha [6] considered the problem of MHD natural convection from an isothermal inclined plate embedded in a thermally stratified porous medium. Elabashbeshy [7] studied heat and mass transfer along a vertical plate in the presence of a magnetic field. Chamkha and Khaled [8] investigated the problem of coupled heat and mass transfer by hydromagnetic free convection from an inclined plate in the presence of internal heat generation or absorption. Chen [9] studied the heat and mass transfer characteristics of MHD natural convection flow over an inclined surface with variable wall temperature and concentration. Rashad [10] studied heat and mass transfer by MHD free convection over a vertical flat plate embedded in a porous medium. Rashad et al. [11] studied the problem of the magnetohydrodynamic free convective heat and mass transfer of a fluid adjacent to a vertical stretching surface embedded in a porous medium. Chamkha et al. [12] studied the coupled heat and mass transfer by MHD natural convection boundary-layer flow over a permeable truncated cone with variable surface temperature and concentration.

In all these studies, the Soret and Dufour effects are assumed to be negligible. Such effects are significant when density differences exist in the flow regime. For example, when species are introduced at a surface in the fluid domain, with different (lower) density than the surrounding fluid, both Soret and Dufour effects can be significant. Also, when heat and mass transfer occur simultaneously in a moving fluid, the relations between the fluxes and the driving potentials are of a more intricate nature. It has been found that an energy flux can be generated not only by temperature gradients but by composition gradients as well. The energy flux caused by a composition gradient is called the Dufour or diffusion-thermo effect. On the other hand, mass fluxes can also be created by temperature gradients and this is the Soret or thermal-diffusion effect. The thermal-diffusion (Soret) effect, for instance, has been utilized for isotope separation, and in mixtures between gases with very light molecular weight (H_2, He) and those of medium molecular weight (N_2, air), the diffusion-thermo (Dufour) effect was found to be of such a considerable magnitude that it cannot be ignored (Eckert and Drake [13]). In view of the importance of these above mentioned effects, Dursunkaya and Worek [14] studied diffusion-thermo and thermal-diffusion effects in transient and steady natural convection from a vertical surface, whereas Kafoussias and Williams [15] studied the same effects on mixed free-forced convective and mass transfer boundary-layer flow with temperature-dependent viscosity. Anghel et al. [16] investigated the Dufour and Soret effects on the free convection boundary layer over a vertical surface embedded in a porous medium. Postelnicu [17] studied numerically the influence of a magnetic field on heat and mass transfer by natural convection from vertical surfaces in porous media considering Soret and Dufour effects. Recently, the thermal-diffusion and diffusion-thermo effects on heat and mass transfer by magnetohydrodynamic (MHD) mixed convection stagnation-point flow of a power-law fluid towards a stretching surface in the presence of a magnetic field effect was studied by EL-Kabeir et al. [18].

Hence, the purpose of the present work is to study the coupled heat and mass transfer by MHD natural convection boundary-layer flow over a vertical flat plate with the combined effects of streamwise sinusoidal variations of both the surface temperature and the species concentration in the presence of Soret and Dufour effects. The governing boundary-layer equations have been transformed into a non-similar form, and these have been solved numerically. The effects of magnetic field, Soret and Dufour, combined buoyancy parameter, and the relative amplitude of the surface temperature and species concentration variations on the velocity, temperature, and concentration profiles as well as the surface shear stress, rate of heat transfer, and the rate of mass transfer have been shown graphically and are discussed.

2. Governing Equations

Consider steady, laminar, heat and mass transfer by natural convection and boundary-layer flow of a viscous, incompressible and electrically conducting fluid along a vertical flat plate with the combined effects of streamwise sinusoidal variations of both the surface temperature and the species concentration in the presence of Soret and Dufour effects. The heated surface of the plate is maintained at a steady temperature and steady concentration $T = T_\infty + (T_w - T_\infty)(1 + a\sin(\pi\bar{x}/L))$, $C = C_\infty + (C_w - C_\infty)(1 + a\sin(\pi\bar{x}/L))$ where T_∞ and C_∞ are the ambient temperature and concentration far away from the surface of the plate and T_w and C_w are the mean temperature and mean concentration with $T_w > T_\infty$ and $C_w > C_\infty$, where a is the relative amplitude of the surface temperature and species concentration variations, and $2L$ is the wave length of the variations. The magnetic Reynolds number is assumed to be small so the induced magnetic field is neglected. In addition, the Hall effect and the electric field are assumed negligible. The small magnetic Reynolds number assumption uncouples the Navier–Stokes equations from Maxwell's equations. With the introduction of Boussinesq and boundary-layer approximations, the equations governing the steady state conservation of mass, momentum, the heat transfer, and the species mass transfer processes can be written as follows (Rees [19] and Roy and Hossain [20]):

$$\frac{\partial \bar{u}}{\partial \bar{x}} + \frac{\partial \bar{v}}{\partial \bar{y}} = 0 \tag{1}$$

$$\bar{u}\frac{\partial \bar{u}}{\partial \bar{x}} + \bar{v}\frac{\partial \bar{u}}{\partial \bar{y}} = \nu\frac{\partial^2 \bar{u}}{\partial \bar{y}^2} + g_1\beta_T(T - T_\infty) + g_1\beta_C(C - C_\infty) - \frac{\sigma B_0^2}{\rho}\bar{u} \tag{2}$$

$$\bar{u}\frac{\partial T}{\partial \bar{x}} + \bar{v}\frac{\partial T}{\partial \bar{y}} = \alpha\frac{\partial^2 T}{\partial \bar{y}^2} + \frac{D_m K_T}{c_s c_p}\frac{\partial^2 C}{\partial \bar{y}^2} \tag{3}$$

$$\bar{u}\frac{\partial C}{\partial \bar{x}} + \bar{v}\frac{\partial C}{\partial \bar{y}} = D_m\frac{\partial^2 C}{\partial \bar{y}^2} + \frac{D_m K_T}{T_m}\frac{\partial^2 T}{\partial \bar{y}^2} \tag{4}$$

where $(\bar{u}, \bar{v})$ are the velocity components along the $(\bar{x}, \bar{y})$ directions. Here T and C are the fluid temperature, and species concentration, respectively. While g_1, ρ, α, D_m, β_T, and β_C are the gravitational acceleration, kinematic viscosity, thermal diffusivity, mass diffusivity, coefficient of thermal expansion, and coefficient of concentration of expansion, respectively. Then σ and B_0 are the electrical conductivity and magnetic induction, respectively, while c_p, T_m, K_T, and c_s are the specific heat at constant pressure, mean fluid temperature, thermal diffusion ratio, and concentration susceptibility.

The corresponding boundary conditions for this problem can be written as:

$$\bar{u} = 0, \bar{v} = 0, T = T_\infty + (T_w - T_\infty)\theta_w(\bar{x}), C = C_\infty + (C_w - C_\infty)\phi_w(\bar{x}) \text{ at } \bar{y} = 0 \tag{5a}$$

$$\bar{u} = 0, T = T_\infty, C = C_\infty \quad \text{as} \quad \bar{y} \to \infty \tag{5b}$$

It is convenient to non-dimensionalize and transform Eqs. (1) through (4) by using

$$x = \frac{\bar{x}}{L}, \bar{u} = \frac{\nu Gr_L^{1/2}}{L}u, \bar{v} = \frac{\nu Gr_L^{1/4}}{L}v, y = \frac{Gr_L^{1/4}}{L}\bar{y}, \theta = \frac{T - T_\infty}{T_w - T_\infty}$$
$$\phi = \frac{C - C_\infty}{C_w - C_\infty}, Gr_L = Gr_T + Gr_C = \frac{g_1\beta_T(T_w - T_\infty)L^3}{\nu^2} + \frac{g_1\beta_C(C_w - C_\infty)L^3}{\nu^2} \tag{6}$$

Substituting Eqs. (6) into Eqs. (1)–(5) yields the following non-similar equations and boundary conditions:

$$\frac{\partial u}{\partial x} + \frac{\partial v}{\partial y} = 0 \tag{7}$$

$$u\frac{\partial u}{\partial x} + v\frac{\partial u}{\partial y} = \frac{\partial^2 u}{\partial y^2} + (1 - w)\theta + w\phi - Hau \tag{8}$$

$$u\frac{\partial \theta}{\partial x} + v\frac{\partial \theta}{\partial y} = \frac{1}{\Pr}\frac{\partial^2 \theta}{\partial y^2} + D_f\frac{\partial^2 \phi}{\partial y^2} \tag{9}$$

$$u\frac{\partial \phi}{\partial x} + v\frac{\partial \phi}{\partial y} = \frac{1}{Sc}\frac{\partial^2 \phi}{\partial y^2} + S_r\frac{\partial^2 \theta}{\partial y^2} \tag{10}$$

$$u = 0, v = 0, \theta = 1 + a\sin(\pi x), \phi = 1 + a\sin(\pi x) \text{ at } y = 0 \tag{11a}$$

$$u = 0, \theta = 0, \phi = 0 \quad \text{as} \quad y \to \infty \tag{11b}$$

where $Ha = \sigma B_0^2 L^2/\mu Gr_L^{1/2}$ is the Hartmann number, $\Pr = \upsilon/\alpha$ and $Sc = \upsilon/D_m$ are the Prandtl number and Schmidt number, respectively. $D_f = D_m k_T(C_w - C_\infty)/\nu c_p c_s(T_w - T_\infty)$ is the Dufour number, $S_r = D_m k_T(T_w - T_\infty)/\upsilon T_m(C_w - C_\infty)$ is the Soret number, and $w = Gr_C/(Gr_T + Gr_C) = N/(1 + N)$ is the combined buoyancy parameter where $N = Gr_C/Gr_T$ measures the relative importance of solutal and thermal diffusion in causing the density changes which drive the flow. It is to be noted that $N = 0$ (i.e., $w = 0$) corresponds to no species diffusion and $N \to \infty$ (i.e., $w \to 1$) to no thermal diffusion. Positive values of N correspond to both effects combining to drive the flow whereas negative values correspond to opposing effects from these two diffusing components.

As the equations are two-dimensional, we define a stream function ψ in the usual way $u = \partial\psi/\partial y$, $v = -\partial\psi/\partial x$ and therefore, Eq. (7) is satisfied automatically. Guided by the familiar non-similar form corresponding to both a uniform surface temperature and concentration, we use the substitution

$$\xi = x, \ \eta = y/\xi^{1/4}, \ \psi = \xi^{3/4}f(\xi,\eta), \ \theta = g(\xi,\eta), \ \phi = h(\xi,\eta) \tag{12}$$

into Eqs. (7) through (11) to yield:

$$f''' + \frac{3}{4}ff'' - \frac{1}{2}f'^2 + (1 - w)g + wh - Ha\xi^{1/2}f' = \xi\left(f'\frac{\partial f'}{\partial \xi} - f''\frac{\partial f}{\partial \xi}\right) \tag{13}$$

$$\frac{1}{\Pr}g'' + \frac{3}{4}fg' + D_f h'' = \xi\left(f'\frac{\partial g}{\partial \xi} - g'\frac{\partial f}{\partial \xi}\right) \tag{14}$$

$$\frac{1}{Sc}h'' + \frac{3}{4}fh' + S_r g'' = \xi\left(f'\frac{\partial h}{\partial \xi} - h'\frac{\partial f}{\partial \xi}\right) \tag{15}$$

The transformed boundary conditions become:

$$f(\xi,0) = 0, \qquad f'(\xi,0) = 0, \qquad g(\xi,0) = 1 + a\sin(\pi\xi), \qquad h(\xi,0) = 1 + a\sin(\pi\xi)$$
$$f'(\xi,\infty) = g(\xi,\infty) = h(\xi,\infty) = 0 \tag{16}$$

The physical quantities of principle interest are the surface shear stress, rate of heat transfer, and the rate of mass transfer, respectively. These can be written as

$$\tau_w = \mu\left(\partial\bar{u}/\partial\bar{y}\right)_{\bar{y}=0}, q_w = -k\left(\partial T/\partial\bar{y}\right)_{\bar{y}=0}, m_w = -D_m\left(\partial C/\partial\bar{y}\right)_{\bar{y}=0} \tag{17}$$

Using the variables (6), (12) and the boundary conditions (16) into Eqs. (17), we get

$$\tau_w = f''(\xi,0),\ q_w = -g'(\xi,0),\ m_w = -h'(\xi,0)$$

3. Numerical Method

The problem represented by Eqs. (13)–(16) is nonlinear and has no closed-form solution. Therefore, it must be solved numerically. The implicit, tri-diagonal, finite-difference method discussed by Blottner [21] has proven to be adequate for the accurate solution of boundary-layer equations. For this reason, it is adopted in this work. All first-order derivatives with respect to ξ are replaced by two-point backward difference quotients while the derivatives with respect to η are discretized using three-point central-difference quotients and, as a consequence, a set of algebraic equations results at each line of constant ξ. These algebraic equations are then solved by the well-known Thomas algorithm (see Blottner [21]) with iteration to deal with the non-linearities of the problem. When the solution at a specific line of constant ξ is obtained, the same solution procedure is used for the next line of constant ξ. This marching process continues until the desired value of ξ is reached. At each line of constant ξ, when *f′* is known, the trapezoidal rule is used to solve for *f*. The convergence criterion employed was based on the relative difference between the current and the previous iterations. When this difference reached 10^{-5}, the solution was assumed converged and the iteration procedure was terminated. Constant step sizes in the ξ direction were used whereas variable step sizes in the η direction were utilized in order to accommodate the sharp changes in the dependent variables especially in the immediate vicinity of the truncated cone surface. The (ξ, η) computational domain consisted of 1001 and 196 points, respectively. The initial step sizes in $\Delta\xi_1$ and $\Delta\eta_1$ were taken to be equal to 2×10^{-2} and 10^{-3}, respectively, and the growth factor for the η direction was taken to be 1.0375. This gave $\xi_\infty = 20$ and $\eta_\infty = 35$. These values were found to give accurate grid-independent results as verified by the comparisons mentioned below.

In order to access the accuracy of the numerical results, a comparison with previously published work for ($Ha = D_f = S_r = 0$) is performed. This comparison is presented in Fig. 1. It is

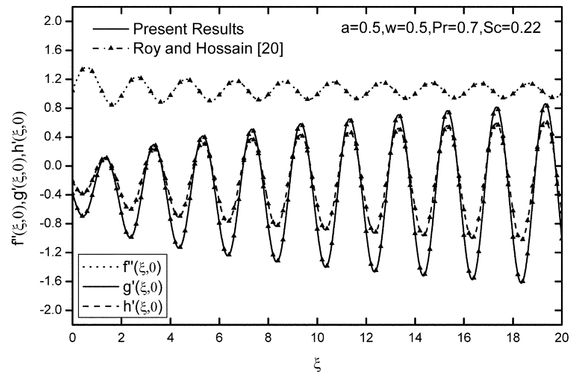

Fig. 1. Comparison between present work and Roy and Hossain [20] for Ha = 0.0, S_r = 0.0, and D_f = 0.0.

obvious from this figure that excellent agreement between the results exist. This favorable comparison lends confidence in the graphical results reported in the next section.

4. Results and Discussion

In this section, a representative set of numerical results for the velocity, temperature, and concentration profiles as well as the local skin-friction coefficient, local Nusselt number, and the local Sherwood number is presented graphically in Figs. 2 through 13. These results illustrate the effects of the Hartmann number Ha, relative amplitude of the surface temperature, and species concentration variations a, Dufour number D_f, and the Soret number S_r. Throughout the calculations, the conditions are intended for a fluid with a Prandtl number Pr = 0.7 which represents air at 20 °C and 1 atmosphere, polluted by hydrogen (Sc = 0.22). The values of the corresponding Dufour number and Soret number are chosen in such a way that their product is constant provided the mean temperature T_m is kept constant as well.

Figures 2 to 4 present typical profiles for the velocity along the plate f', temperature g, and concentration h for two different values of the Hartmann number Ha and various values of the relative amplitude of the temperature and species concentration variations a, respectively. Application of a magnetic field normal to the flow of an electrically conducting fluid gives rise to a resistive force called the Lorentz force which acts in the direction opposite to that of the flow. This resistive force tends to slow down the motion of the fluid along the plate and causes increases in its temperature and solute concentration. On other hand, it is seen that all of the velocity, temperature, and concentration profiles increase significantly with increases in the relative amplitude of the temperature and species concentration variations a. This arises because relatively high surface temperatures and species concentration induce relatively large upward fluid velocities with the consequent increase in the rate entrainment into the boundary layer.

Figures 5 to 7 illustrate the effects of the Hartmann number Ha and the relative amplitude of the temperature and species concentration variations a on the development of the surface shear stress (or $f''(\xi, 0)$), rate of heat transfer (or $g'(\xi, 0)$), and the rate of mass transfer (or $h'(\xi, 0)$), respectively. It can be observed that there are two opposite behaviors for the local skin-friction coefficient and both

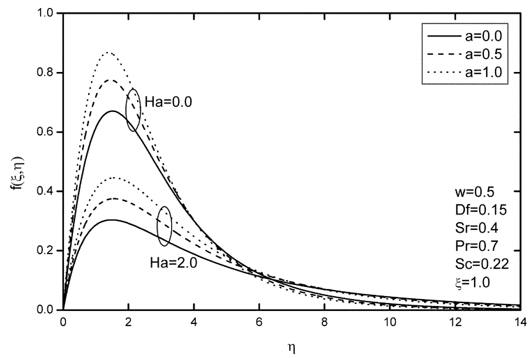

Fig. 2. Effects of *Ha* and *a* on velocity profiles.

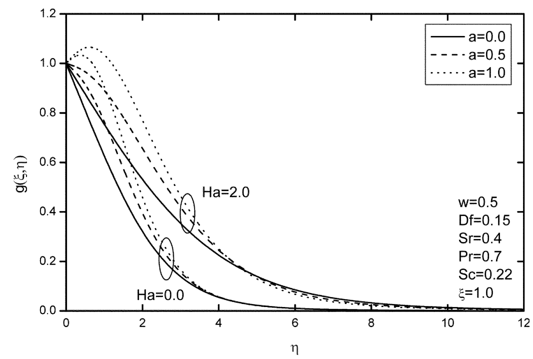

Fig. 3. Effects of *Ha* and *a* on temperature profiles.

the local Nusselt number and the local Sherwood number. These behaviors are represented by the increases in both of the rates of heat and mass transfer and the decrease in the surface shear stress as a result of increasing the Hartmann number. Further, it can be seen that the increase of the relative amplitude of the temperature and species concentration variations a causes increases in all of the surface shear stress, rate of heat transfer, and the rate of mass transfer. Moreover, it is also observed that the amplitude of oscillation of the shear stress curves decays slowly while the amplitudes of oscillations of both the rate of heat transfer and the rate of mass transfer increase as ξ increases. Indeed, the curves in Figs. 5–7 show that whatever the value of a, there will always be a value of ξ beyond which some part of the rate of heat transfer and the rate of mass transfer curves between successive surface temperature maxima will be positive.

Figures 8 to 10 show the effects of the Dufour number D_f and the Soret number S_r on the velocity, temperature, and concentration profiles for two values of the combined buoyancy parameter w, respectively. It should be noted that the parameter w measures the relative importance of solutal and thermal diffusion in causing the density changes which drive the flow. It is also to be noted that the condition $w = 0$ corresponds to no species diffusion and the condition as $w \to 1$ corresponds to

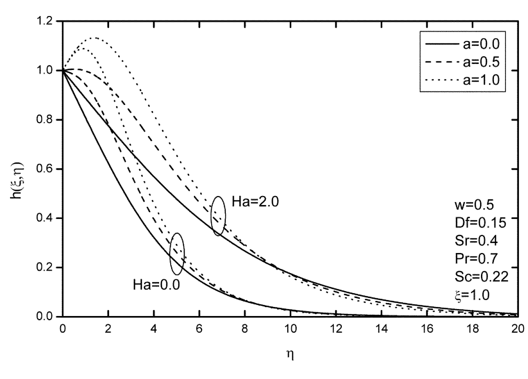

Fig. 4. Effects of *Ha* and *a* on concentration profiles.

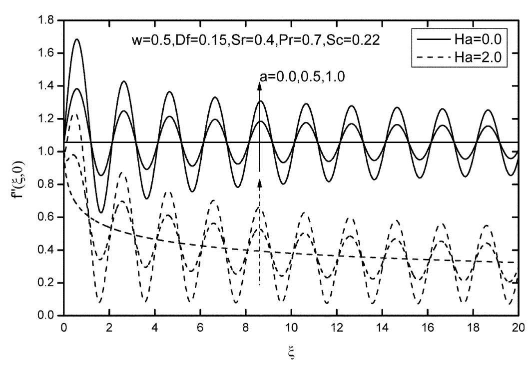

Fig. 5. Effects of *Ha* and *a* on the surface shear stress.

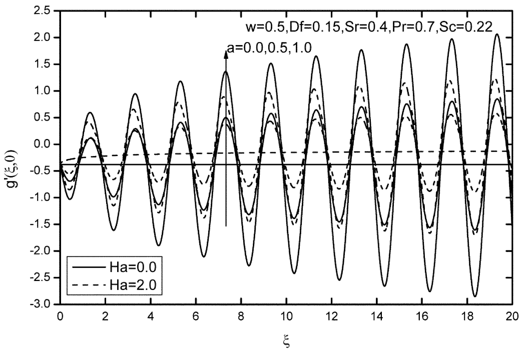

Fig. 6. Effects of *Ha* and *a* on the rate of heat transfer.

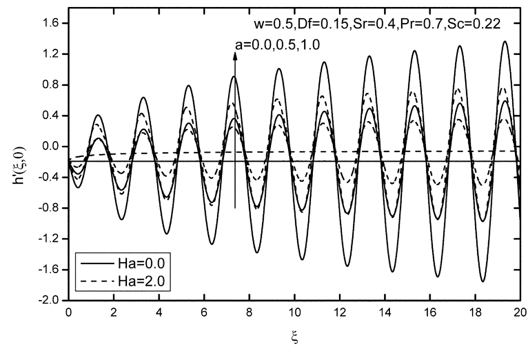

Fig. 7. Effects of *Ha* and *a* on the rate of mass transfer.

no thermal diffusion. Increasing the combined buoyancy parameter w has a tendency to accelerate the flow causing its velocity to increase while it produces decreases in both the temperature and concentration profiles. It is also observed that as w increases, the distinctive peak or maximum point in the velocity profile tends to move away from the surface. On other hand, it is noticed that as S_r increases (or D_f decreases) the concentration profiles increase while the temperature profiles decrease. This behavior is a direct consequence of the Soret effect which produces a mass flux from lower to higher solute concentration driven by the temperature gradient. Moreover, when $w = 1$ and D_f is high enough, the thermal and the solutal buoyancy forces combine their actions to enhance the convection velocity, which leads to an increase in the velocity of the fluid, whereas the opposite behavior is predicted when $w = 0$.

The effects of both the Dufour number D_f and the Soret number S_r on the development of the surface shear stress $f''(\xi, 0)$, rate of heat transfer $g'(\xi, 0)$, and the rate of mass transfer $h'(\xi, 0)$ for various values of the buoyancy parameter w are displayed in Figs. 11–13, respectively. From these figures, it can observed that as the Dufour number D_f increases (S_r decreases), both the surface shear stress and the rate of heat transfer increase slightly, while the rate of mass transfer decreases weakly.

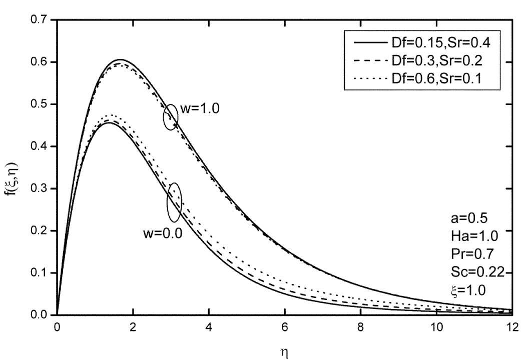

Fig. 8. Effects of w, D_f, and S_r on velocity profiles.

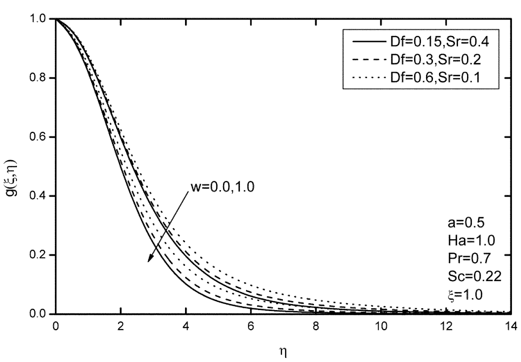

Fig. 9. Effects of w, D_f, and S_r on temperature profiles.

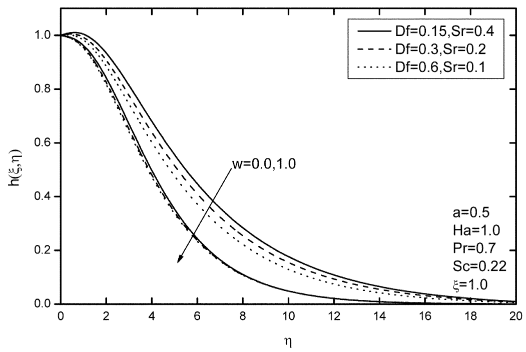

Fig. 10. Effects of w, D_f, and S_r on concentration profiles.

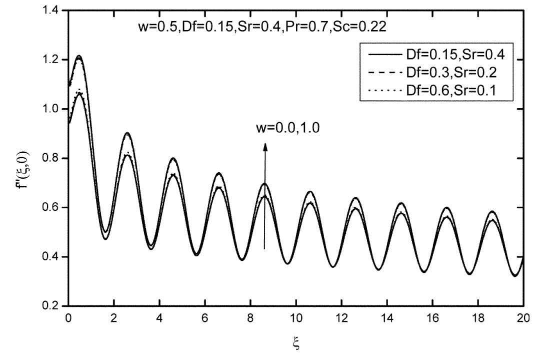

Fig. 11. Effects of w, D_f, and S_r on the surface shear stress.

This is because either an increase in the temperature difference or a decrease in the concentration difference leads to an increase in the value of D_f resulting in trends similar to the above observation. Similarly, either an increase in the concentration difference or a decrease in the temperature difference leads to an increase in the value of the Soret number S_r. Therefore, increasing the parameter S_r causes decreases in the surface shear stress $f''(\xi, 0)$ and the rate of heat transfer $g'(\xi, 0)$ while it produces increases in the rate of mass transfer $h'(\xi, 0)$. However, it should be mentioned that the rate of shear stress increases with increasing values in the buoyancy parameter w whereas the opposite effect is produced with the rate of heat transfer and the rate of mass transfer. In addition, for a given value of w, the amplitude of oscillation of the local surface shear stress curves are higher close to $\xi = 0$ and decreases as ξ increases. On the other hand, the amplitudes of oscillations of both the rate of heat transfer and the rate of mass transfer increase as ξ increases. Finally, it can be seen that the effect of the buoyancy parameter w on the rate of heat transfer and the rate of mass transfer are considerably less because the flow is induced almost entirely by thermal buoyancy and produces a very effective species diffusion at very low concentration.

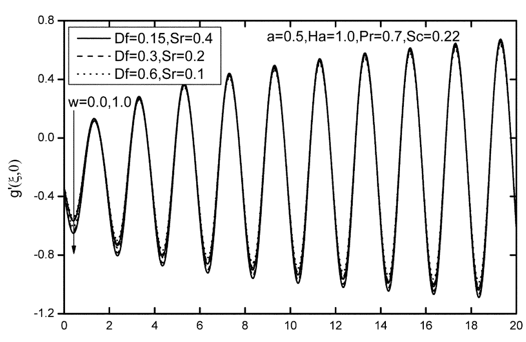

Fig. 12. Effects of w, D_f, and S_r on the rate of heat transfer.

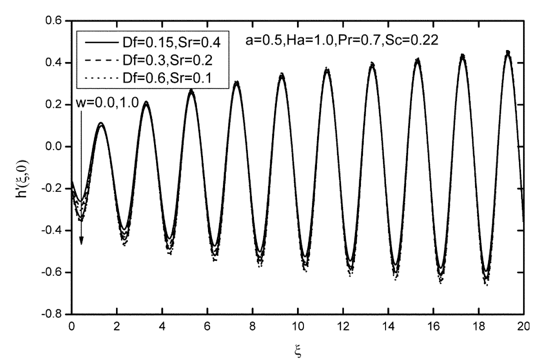

Fig. 13. Effects of w, D_f, and S_r on the rate of mass transfer.

5. Conclusion

The problem of coupled heat and mass transfer by MHD free convective boundary-layer flow along a vertical flat plate with the combined effects of streamwise sinusoidal variations of both the surface temperature and the species concentration in the presence of magnetic field, Soret, and Dufour effects is considered. A set of non-similar governing differential equations was obtained and solved numerically by an implicit finite-difference methodology. Comparisons with previously published works on a special case of the general problem was performed and the results were found to be in excellent agreement. A representative set of numerical results for the velocity, temperature, and concentration profiles as well as the surface shear stress, rate of heat transfer, and the rate of mass transfer was presented graphically and discussed. It was found that both the rate of heat transfer, and the rate of mass transfer increased while the shear stress decreased as the magnetic Hartmann number was increased. Furthermore, it was found that owing to the increase of the relative amplitude of the temperature and species concentration variations, the surface shear stress, rate of heat transfer, and the rate of mass transfer all increased. In addition, it was observed that both the shear stress and the rate of mass transfer were found to increase slightly while the rate of mass transfer decreased as the Dufour number increased or the Soret decreased. It should be mentioned that the shear stress increased with increases in the value of the combined buoyancy parameter whereas the opposite effect was obtained for the rates of heat and mass transfer.

Literature Cited

1. Gebhart B, Jaluria Y, Mahajan RL, Sammakia B. Buoyancy-induced flow and transport. Hemisphere; 1998.
2. Callahan GD, Marner WJ. Transient free convection with mass transfer on an isothermal vertical flat plate. Int J Heat Mass Transf 1976;19:165–174.
3. Soundalgekar VM, Wavre PD. Unsteady free convection flow past an infinite vertical plate with constant suction and mass transfer. Int J Heat Mass Transf 1977;20:1363–1373.
4. Soundalgekar VM. Effects of mass transfer and free convection currents on the flow past an impulsively started vertical plate. ASME J Appl Mech 1979;46:757–760.
5. Shanker B, Kishan N. The effects of mass transfer on the MHD flow past an impulsively started infinite vertical plate with variable temperature or constant heat flux. J Eng Heat Mass Transf 1997;19:273–278.
6. Chamkha AJ. Hydromagnetic natural convection from an isothermal inclined surface adjacent to a thermally stratified porous medium. Int J Eng Sci 1997;34:975–986.
7. Elabashbeshy EMA. Heat and mass transfer along a vertical plate with variable temperature and concentration in the presence of magnetic field. Int J Eng Sci 1997;34:515–522.
8. Chamkha AJ, Khaled ARA. Similarity solutions for hydromagnetic simultaneous heat and mass transfer by natural convection from an inclined plate with internal heat generation or absorption. Heat Mass Transf 2001;37:117–123.
9. Chen C-H. Heat and mass transfer in MHD flow by natural convection from a permeable, inclined surface with variable wall temperature and concentration. Acta Mechanica 2004;172:219–235.
10. Rashad AM. Influence of radiation on MHD free convection from a vertical flat plate embedded in porous media with thermophoretic deposition of particles. Commun Nonlinear Sci Numer Simul 2008;13:2213–2222.

11. Rashad AM, Modather M, Chamkha AJ. MHD free convective heat and mass transfer of a chemically-reacting fluid from radiate stretching surface embedded in a saturated porous medium. Int J Chem Reactor Eng 2011;9:1–15.
12. Chamkha AJ, Rashad AM, Al-Mudhaf HF. Heat and mass transfer from truncated cones with variable wall temperature and concentration in the presence of chemical reaction effects. Int J Numer Meth Heat Fluid Flow 2012;22:357–376.
13. Eckert ERG, Drake RM. Analysis of heat and mass transfer. McGraw-Hill; 1972.
14. Dursunkaya Z, Worek WM. Diffusion-thermo and thermal diffusion effects in transient and steady natural convection from a vertical surface. Int J Heat Mass Transf 1992;35:2060–2065.
15. Kafoussias NG, Williams EM. Thermal-diffusion and diffusion-thermo effects on free convective and mass transfer boundary layer flow with temperature dependent viscosity. Int J Eng Sci 1995;33:1369–1376.
16. Anghel M, Takhar HS, Pop I. Dufour and Soret effects on free convection boundary layer over a vertical surface embedded in a porous medium. J Heat Mass Transf 2000;43:1265–1274.
17. Postelnicu A. Influence of a magnetic field on heat and mass transfer by natural convection from vertical surfaces in porous media considering Soret and Dufour effects. Int J Heat Mass Transf 2004;47:1467–1472.
18. EL-Kabeir SMM, Chamkha AJ, Rashad AM. Heat and mass transfer by MHD stagnation-point flow of a power-law fluid towards a stretching surface with radiation, chemical reaction and Soret and Dufour effects. Int J Chem Reactor Eng 2010;8:1–18.
19. Rees DAS. The effect of steady streamwise surface temperature variations on vertical free convection. Int J Heat Mass Transf 1999;42:2455–2464.
20. Roy NC, Hossain MA. Numerical solution of a steady natural convection flow from a vertical plate with the combined effects of streamwise temperature and species concentration variations. Heat Mass Transf 2010;46:509–522.
21. Blottner FG. Finite-difference methods of solution of the boundary-layer equations. AIAA J 1970;8:193–205.

□♦ ♦ ♦□